Article ID: 1006-8775(2017) 02-0177-14

ANALYSIS OF THE MICROPHYSICAL STRUCTURE OF RADIATION FOG IN XUANEN MOUNTAINOUS REGION OF HUBEI, CHINA

FEI Dong-dong (费冬冬)[1, 2], NIU Sheng-jie (牛生杰)[1], YANG Jun (杨 军)[1]
(1. Collaborative Innovation Center of Atmospheric Environment and Equipment Technology, School of Atmospheric Physics, Nanjing University of Information Science & Technology, Nanjing 210044 China;
2. MCC Huatian Engineering & Technology Co. Ltd., Nanjing 210019 China)

Abstract: Based on data of radiation fog events in Xuanen, Hubei province, 2010, this paper analyzes the microphysical process and evolution characteristics of radiation fogs with complicated substrate in the upper and middle reaches of the Yangtze River, and compares them with findings in other areas. Results are as follows: radiation fog in Xuanen is evidently weaker in droplet number concentration and liquid water content than land fogs in other areas. Its liquid water content fluctuates obviously, 0.01g/ m3 with visibility of 1,000 meters, which is quite different from that in urban areas, but similar to the Nanling Mountains. Bi-modal droplet distribution is likely to occur in Xuanen mountain radiation fog (MRF) events. Statistical analysis shows that the observed droplet size distribution can be piecewise described well by the Gamma distribution. There is a positive correlation between liquid water content, fog droplet concentration and mean radius, especially in the development and dissipation stage. Condensation growth and droplet evaporation are major processes of Xuanen MRF. The dissipation time coincided with the time when the grass temperature reached the peak value, which indicated that dew evaporation is a key role in maintaining Xuanen MRF. In the early stage of dense fog's growth, droplets with diameter of over 20 micrometers can be observed with visibility of 800-1,000m, which might be caused by the transportation of low cloud droplets to earth's surface by turbulence. Big droplets in the initial stage correspond to higher water content, leading to the higher observed value of water content of Xuanen MRF.

Key words: mountainous radiation fog; fog microphysics; upper and middle reaches of the Yangtze River
CLC number: P466 **Document code:** A
doi: 10.16555/j.1006-8775.2017.02.006

1 INTRODUCTION

Fog is an aerosol system composed of suspended water droplets or ice crystals near the Earth's surface, created by the condensation of water vapor in near-surface air (Gultepe et al. [1]). As a common disastrous weather event, fog has over the years severely affected normal transportation and electric transmission, causing huge damage to national economy and properties. Of economic losses caused by natural disasters, 70 percent involves drought, flood, hail and fog (Guo and Zheng [2]). On the other hand, fog is usually considered a positive entity, and may add much needed moisture to arid ecosystems, thus benefiting tea production in mountainous areas and growth of tropical rainforest (Bendix et al.[3]; Niu et al.[4]).

In summary of fog research, Gultepe and Niu arrived at the conclusion that the radiation-related land fog, mainly including radiation fog and advection-radiation fog, cost most study efforts and are best understood [1, 5]. It is found that fog visibility is closely related to liquid water content (Pinnick et al.[6]). By introduction of fog droplet concentration as a parameter into the expression of visibility, Gultepe and Milbrandt explain the effect of changing concentration to the oscillation of visibility [7]. According to García-García, fog layer has a heterogeneous characteristic, with a possible variation range of two orders of magnitude[8-10], and liquid water content of less than 0.5 g/m^3 (Fuzzi et al. [11]). Vertically, after the formation of the fog, the layer's maximum cooling separated from the surface because of the warming of the ground. The cooling produces liquid water, which is depleted by turbulence near the surface. The influence of turbulence on the liquid water budget decreases with height and is more significant for shallow fogs than for deep fogs. Mean radius and liquid water content of droplets are increasing with the height near the surface, so does the fog droplet spectra width (Goodman et al.[12]; Zhou et al.[13]). As to fog droplet concentration, urban areas rank the top,

Received 2015-10-08; **Revised** 2017-03-29; **Accepted** 2017-05-15
Foundation item: National Natural Science Foundation of China (41375138, 41305120, 41275151); Natural Science Foundation of Jiangsu Province, China (BK20130988); Specialized Research Fund for the Doctoral Program of Higher Education (20133228120002); Graduate Student Innovation Plan at the Universities of Jiangsu province (N0782002211)
Biography: FEI Dong-dong, Ph. D., primarily undertaking the assessment of atmospheric environment.
Corresponding author: FEI Dong-dong, e-mail: feidd_12@nuist.edu.cn

mountainous regions take the second place, and sea fog comes the last. The case is opposite for mean diameter. Mean diameter and fog droplet concentration are negatively correlated (Huang et al.[14]; Tang et al.[15]); liquid water content is positively correlated with mean radius, particularly maximum diameter. Important overseas study of valley fog includes Pilié's research of Chemung valley fog in New York, Holets and Swanson's research of California valley fog, Fitzjarrald and Lala's research of Hudson valley fog, and Wobrock's research of Po valley fog in Italy[16-20]. These researches offer a preliminary understanding of formation mechanism of valley fog: warming downdraft under high pressure, radiation cooling and mountain breeze circulation promote valley fog's formation, and advection plays a more important part in the formation of Po valley fog. Important domestic study of mountainous fog includes Nanling Mountains in Guangdong province (Deng et al.[21]), Xishuangbanna in Yunnan Province, Lou Mountain in Guizhou Province, and Chongqing (He et al.[22]). It is found that orographic uplift is the major cause of formation of fog in Nanling Mountains (Shi et al.[23]). Compared to ten years ago, fog droplet concentration in Chongqing and Xishuangbanna increases significantly and mean radius decreases, which mainly results from the influence of urbanization. When pollution worsens, aerosol particle concentration increases, causing more fog droplets.

The upper and middle reaches of the Yangtze River are fog-prone areas in China, with 20–106 fog days every year (Wu et al.[24]). For instance, the radiation fog days in Enshi are up to 103 days every year, and a radiation fog event lasted nine days in November 2007. Statistical analysis showed that there are 60 fog days in Chongqing and 50 fog days in Jinzhou every year, and there are more than thirty fog-prone sections in Yichang city. Traffic accidents often occurred when radiation fog events appeared at high altitude in the early morning. On 22 March, 18 and 24 April, 2009, navigation through five-step ship locks at Three Gorges on the Yangtze River was unusually long, caused by radiation fogs in this region. Radiation fog in this area is characterized by high frequency, extensive influence, and severe destruction, making radiation fog study a particularly pressing task. In the winter of 2010, using the FM-100 droplet spectrometer, a comprehensive field observation of mountainous fog was conducted in Xuanen, Hubei Province. Fog droplet size distribution data with a resolution of 1 Hz and particle size ranging from 2 to 50 μm were continuously obtained, in attempt to make an in-depth analysis of the correlation between the microphysical process and microphysical properties of valley fog in this area.

This paper examines three fog events observed in Xuanen, with an emphasis on variability and mutual relationships between key microphysical properties: mean radius ($\bar{r}$), number concentration (N), and liquid water content (LWC). The rest of the paper is organized as follows. Section 2 introduces the observation and data. Section 3 and 4 are the results, including comparison of microphysical properties, microphysical relationships and evolution of fog droplet size distribution. Conclusion is presented in section 5.

2 OBSERVATIONS

2.1 *Sites and instruments*

The comprehensive field observation of mountainous radiation fog ("MRF" below) in December, 2010 was conducted in Xuanen, Hubei Province (30°N, 109.4°E; 530 m above sea level). The principal measurement site was Xuanen meteorological bureau and at the site indicated by a black circle "O" in Fig.1. Located at southwest of Hubei Province, Xuanen is in an extended part of the Yunnan-Guizhou Plateau at the intersection between Wuling Mountains, the branch of Miaoling Mountains and Qiyue Mountain, the northern section of Dalou Mountains, the boundary between second and third terrain of China and the boundary between Sichuan Basin and the Middle-Lower Yangtze plains. The observation site is surrounded by mountains with high vegetation coverage. This observation includes surface visibility, boundary layer meteorological elements, and fog droplet size distribution.

The XLS-Ⅱ tethersonde system was used to probe the planetary boundary layer (PBL). The measurements of temperature, pressure, humidity, wind speed and direction at various heights, with resolutions of less than 1 km, are 0.3 °C, 0.1 hPa, 5%, 0.25 m s^{-1}, and 10°, respectively. In general, observations were performed every 3 h on fog-free days, and every 1 h on fog days. The fog droplets spectra were obtained by a FM-100 droplet spectrometer (Gultepe and Milbrandt [7]). The instrument was set up 1 m above the ground. Visibility was automatically measured and recorded every 30 seconds by the vpf730 visibility meter, a product of Biral, UK. The relative accuracy of the instrument is ≤±10%/20% when the visibility is less/more than 16 km. Surface meteorological quantities (temperature, relative humidity, wind speed and direction) were observed with a ZQZ-CⅢ automatic weather station, a product of the Radio Scientific Research Institute, Jiangsu Province, China.

2.2 *Data*

This observation consists of three events. Table 1 shows major macro features of three events. Fog case 1 took shape around 06:00 LST (LST=UTC+8 h) in the morning; the other fog events form several hours before sunrise. The minimum visibility indicates that Xuanen MRF is obviously weaker in strength than that of urban areas, such as Nanjing (Niu et al.[4]), also weaker than radiation fog of mountain land in Nanling and Xishuangbanna, without any extremely dense fog event. The observed three radiation fog cases lasted for three

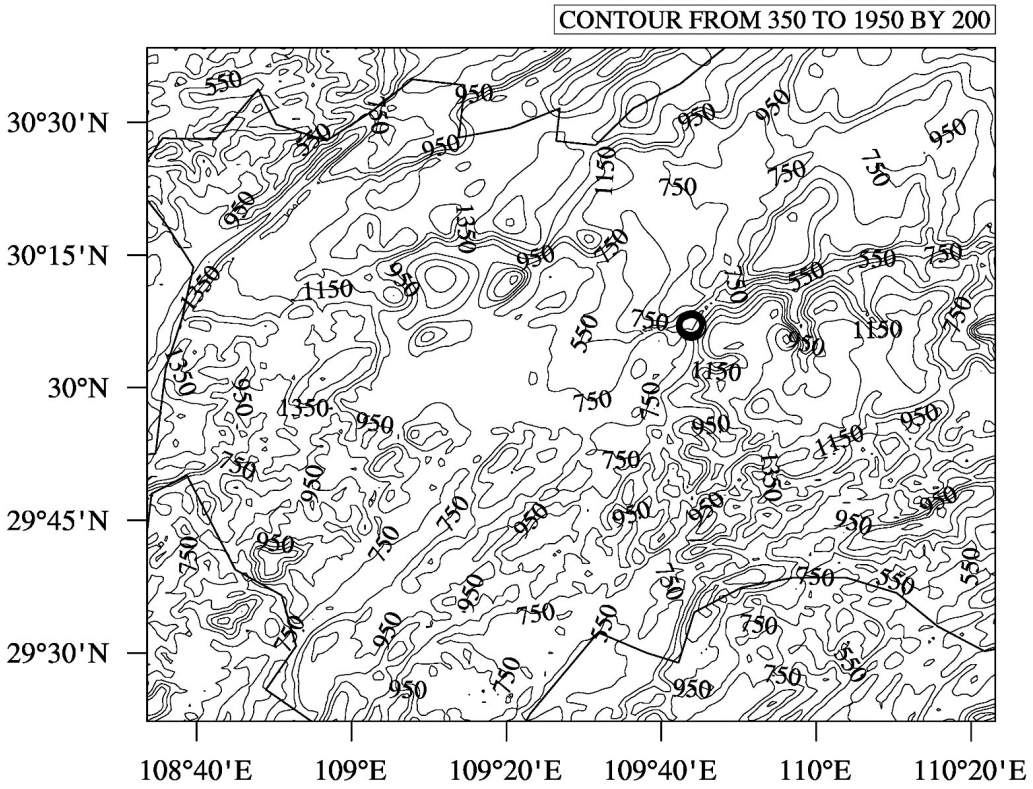

Figure 1. Topography around the Xuanen field site.

Table 1. The Macro-structural features of three fog events in Xuanen in December 2010.

case	Starting and ending time (LST)	Duration (min)	Minimum visibility (m)	Top height of fog (m)	Ground temperature (℃)	Fog top temperature (℃)	Leading wind on the ground (°)	Average wind speed on the ground (m/s)
1	Dec. 9 06:15-09:40	205	170	400–460	3.5–4.0	1.0–2.5	100–180	1.0
2	Dec. 20 02:40-04:50	130	300	400–430	2.5–3.5	1.8–2.0	80–150	0.5
3	Dec. 22 00:30-04:00	150	100	450–560	1.5–3.0	1.9–2.0	80–200	1

hours. The top height of fog reaches 400–600 meters in the mature stage, indicating a vertically strong development of Xuanen MRF, which is well matched in thickness with that of Nanjing, Xishuangbanna and Chongqing, and even thicker than the Po valley fog. The temperature of earth surface and fog top demonstrates that Xuanen fog is warm, and southeast wind is the dominant ground wind during fog event, with a slower wind speed of no more than 1 m/s on average, and instantaneous wind speed of no more than 2 m/s. After dark and before fog takes form, calm wind prevails on the ground. Fig.2 presents variations of ground visibility with time during the three fog events. It is indicated that fog dissipation often occurred before daybreak in this region. Actually, radiation fog is mostly dissipated after sunrise when the surface is heated by solar radiation, leading to rising temperature, increasing saturation vapor pressure, decreasing relative humidity and enhanced visibility.

3 RESULTS OF DATA ANALYSIS

3.1 *Comparison of microphysical properties of mountainous fog*

Table 2 demonstrates microphysical properties of three fog events in Xuanen. For the formula concerning mean radius, fog droplet concentration, and liquid water content, see Niu et al.[5]. Mean N of Xuanen fog events is very small, less than 10/cm^3, far lower than other parts of China, such as 240 –1,518/cm^3 in Nanjing, 700/cm^3 in Beijing (Guo et al.[25]), 47–201/cm^3 in Dayao Mountain, Nanling (Wu et al.[24]), and 81 –315/cm^3 in Mengyang, Yunnan Province. Mean concentration in Chongqing, the mountain city, is 188 –1,749/cm^3, 267/cm^3 on Lou Mountain, Guizhou Province, 256 – 417/cm^3 in Chengdu, Sichuan province, 37/cm^3 in sea fog of Zhoushan (Yang et al.[26]), and 40/cm^3 in sea fog of South China Sea (Zhang et al.[27]), which is lower than observed values in overseas mountain areas, such

as the value of 49 –286/cm^3 in Po valley in Italy. According to the observed value in Chemung River valley in 1970s, the mean concentration of 10/cm^3 is similar to that of Xuanen MRF. Xuanen is located in the northern section of the Yunnan-Guizhou Plateau, which is a clean background area. Low aerosol number concentration might be the major cause of light fog droplet concentration. The maximum value of LWC of these fogs is 0.15, 0.018 and 0.06 g/m^3. The average LWC of obtained Xuanen MRF is 0.000,8 –0.004 g/m^3, smaller than the observed values in Mengyang, Yunnan, Jinghong, Chongqing, mainly because fogs in Nanling Mountains, Guangdong Province and Mengyang are actually formed by low clouds grounded at high altitudes. What has been measured is water content in clouds, which is much more than that of fogs. The maximum diameter of Xuanen MRF is no different from those of other mountain areas in China, mostly between 30μm and 40μm. But compared to sea fogs, it is smaller than that of Zhoushan by 30%, and bigger than the South China Sea fog by 40%.

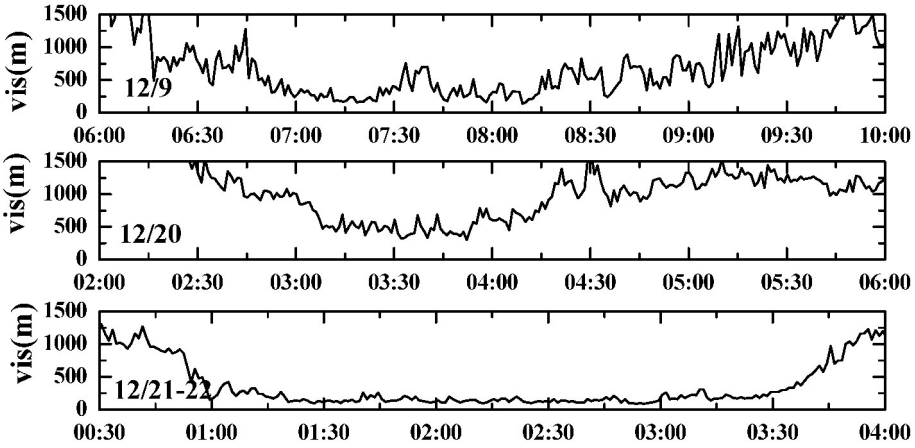

Figure 2. The temporal visibility variations of three fog events in Xuanen in December 2010.

Table 2. Comparison of microphysical properties of the three fog events between Xuanen and other places.

Observation field	case	Minimum Visibility (m)	Concentration N (cm^{-3})	Liquid Water Content LWC(g m^{-3})	Maximum Diameter Dmax(μm)	Average radius $\bar{r}$(μm)
Xuanen mountainous, China	9 Dec. 2010	170	9(1–58)	0.004 (0-0.15)	42.0	4.0
	20 Dec. 2010	300	1(0.5–12)	0.0002(0-0.018)	32.0	1.7
	21-22 Dec. 2010	100	10(0.5–85)	0.0008(0-0.06)	39.0	2.2
Nanling Mountain, China	31 Dec. 1998–2 Jan. 1999		47.3	0.104		6.6
	11-15 Jan. 1999		170.2	0.186		3.7
	18-20 Jan. 1999		78.7	0.166		5.5
	24-28 Feb. 2001		191.4	0.173		4.1
	7-8 Mar. 2001		201.7	0.140		3.6
Yunnan Mengyang Mountain, China	26 Nov. 1997		81.7 (10.9–388.5)	0.082 (0.003–0.258)	41.0 (19.2–78.4)	4.6 (2.3–13.6)
	28 Nov1997		313 (2.2–955.2)	0.116 (0.001–0.568)	40.0 (14.4–80.0)	3.6 (2.0–8.8)
	29 Nov. 1997		315 (16.4–2437.7)	0.174 (0.007–0.667)	31.5 (12.8–60.8)	3.8 (2.0–8.2)
Italy Po River Valley	13-14 Nov. 1994		201	0.266		9.1
	14-15 Nov. 1994		206	0.177		8.8
	16 Nov. 1994		49	0.022		5.8
	21-22 Nov. 1994		57	0.028		8.9
	23 Nov. 1994		135	0.054		4.7
	23-24 Nov. 1994		108	0.115		11.0
	24-25 Nov. 1994		71	0.092		9.3
	28-29 Nov. 1994		284	0.308		–
New York Chemung River Valley	Sept. 1970		10 (1–30)	0.001 (0–0.18)		6.3

Figure 3 displays the average fog droplet spectral distribution in the three cases of radiation fog in Xuanen. Based on the measured data and the Gamma distribution ($n(r) = N_0 r^{\mu} e^{-\lambda r}$, where r, $n(r)$ and b are the droplet radius and the number of droplets per unit volume per unit radius interval, respectively; N_0, λ, and μ are the intercept, slope, and shape parameters, respectively, and the average spectra are fitted by applying the least squares method. As can be seen from Fig.3, in the three fog events, the droplet spectrum is of bi-modal droplet distribution structure, with its second peak located at a diameter of 20 μm. This result is similar with that observed by Pilié[17] and Jeremy[28]. The Gamma distribution, a unimodal function, is quite difficult to well fit this bi-modal droplet distribution. By fitting coefficient R^2, the droplet distribution of the three fog cases was divided into three parts, respectively. The three parts of average spectral distribution can well meet the Gamma distribution, and ideally the optimal degree of fitting results is more than 0.83. Especially in diameters less than 10 μm and more than 20 μm, the optimal degree of fitting results is more than 0.94.

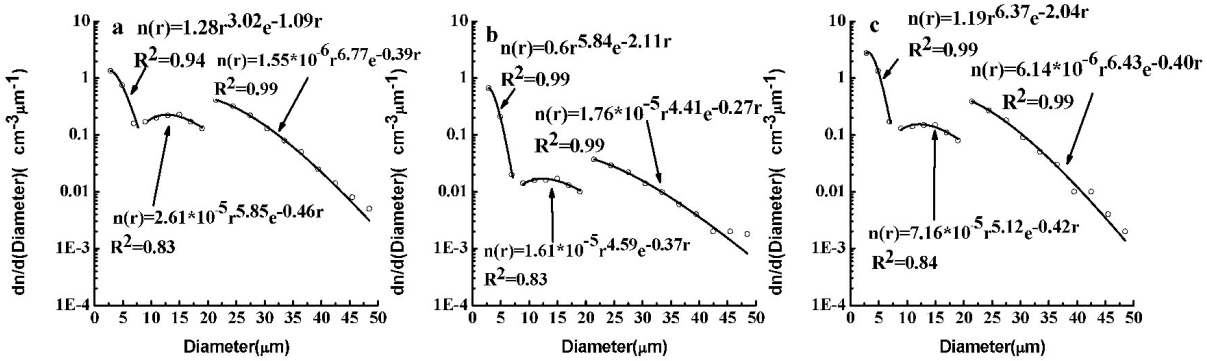

Figure 3. Average droplet spectra of fog case 1, 2, and 3 (a, b, c) in Xuanen in December 2010.

3.2 *Microphysical properties of mountains radiation fog*

Figure 4 shows the correlation between the visibility with N and that with LWC of radiation fog in Xuanen mountainous region, each of which demonstrates a good inverse relationship. Liu et al., (2011) conducted research into finding out the correlation of visibility, N and LWC of dense fog in Nanjing, the findings are as follows: when visibility is between 200 –1,000 m, the N is less than 7/ cm^3,the LWC is less than 0.000,1 g/m^3; when visibility is between 100–200 m, the N is between 7–100/cm^3, LWC is between 0.000,1 –0.005 g/m^3; while the visibility is less than 100 m, N is above 100/cm^3,LWC is more than 0.005 g/m^3 [29]. By comparison, in Xuanen, when the visibility of fog is between 100–200 m, N is 5–85/cm^3; when the visibility is above 200 m, N is 0.3 –63/cm^3, which is remarkably different from the findings in Nanjing. Similarly, when the visibility of radiation fog in Xuanen is between 200–1,000 m, its maximum LWC can reach 0.02 g/m^3. This is similar with the fog feature in Nanling of Guangdong Province. In Nanling, when the visibility is 1,000 m, LWC can be up to 0.015 g/m^3. Mountainous fog in Nanling is actually caused by low clouds at higher altitudes ground. As can be determined from the above analysis, the microphysical quantity of radiation fog in Xuanen mountainous fluctuates greatly in this whole process. When the visibility is about 1,000 m, the LWC can reach about 0.01 g/m^3, which may be a unique phenomenon of mountainous fog.

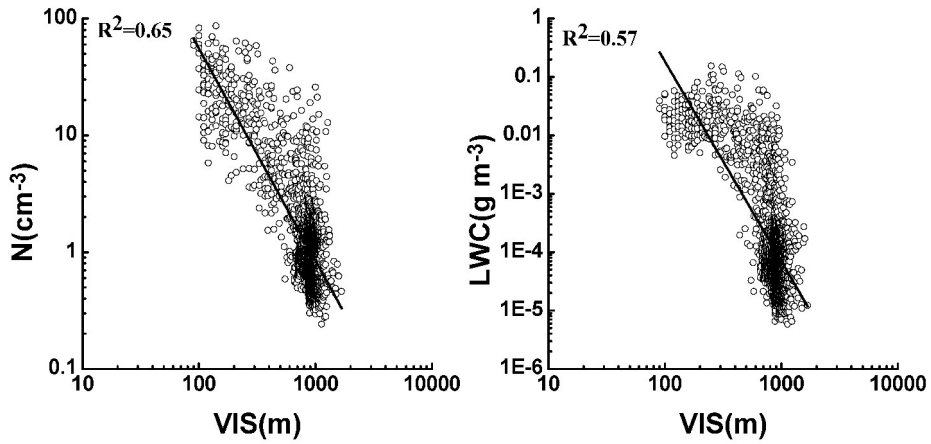

Figure 4. Scatter diagram of visibility relative to the number density of (a) droplets N and (b) LWC in during three fog events.

Figure 5 reflects the correlation between the $\bar{r}$ and N, and between N and LWC in the three cases of radiation fog in Xuanen. Judging from Fig.5a, $\bar{r}$ and N are positively correlated in fog case 1 and 2. The research into the correlation of the microphysical parameter of fog demonstrates that generally the $\bar{r}$ of droplet is inversely proportional to N, and more aerosols result in more droplets and a smaller mean radius when LWC remains unchanged. (Li et al.[30]; Huang et al.[31]; Tang et al.[15]). The analyses of radiation fog in Nanjing by Niu et al, and Lu et al. shows that both $\bar{r}$–N and N-LWC are positively correlated in the process[5,32]. Particularly, at the formation and dissipation stage of fog, they reflect significantly positive correlation, yet at different periods of the mature stage, microphysical quantity correlation portrays different characteristics. The positive correlation of $\bar{r}$–N in fog case 1 and 2 means that N and LWC increase at the same time, which is obvious in Fig.5b; the evaporation to deactivation of the particle may lead to the decrease of N and LWC at the same time; and likewise, the collision and coalescence process will only change N at the same time, and this process tends to destroy the positive correlation of N-LWC. Therefore, the positive correlation of N-LWC indicates the likely dominance of two contrasting processes in Xuanen radiation fogs: particle activation with subsequent condensation growth and droplet deactivation through some droplet evaporation.

On the basis of Fig.5c, we found that the correlation between $\bar{r}$ and N is positive when N is less than 20 /cm^3, and even negative correlation as N more than 20 /cm^3. However, the correlation between N and LWC is well positive in the whole fog case 3. $\bar{r}$ is mainly determined by big droplets, while N is contributed to dominantly by small ones. This means that the number concentration of big droplets has not changed significantly, but more small droplets are reproduced. This can be seen in Fig. 6 which gives the temporal evolutions of big droplets (radius >10 μm) and small droplets (radius ≤10 μm) number concentrations in case 3. It is demonstrated that LWC in case 3 is contributed to dominantly by small ones. Fig.5d shows that the increased rate of LWC is significantly slower than case 1 and 2. Therefore, with non-correlation or even negative correlation between $\bar{r}$ and N, it can also induce a positive correlation between N and LWC but the LWC increase rate may be much smaller than the positive correlation between $\bar{r}$ and N.

It is noteworthy that the dominance of droplet activation with subsequent condensational growth or evaporation does not rule out the roles of other processes completely. In radiation fog events, collection usually is another important process (Niu et al.[5]). The role of collection process in these three fog cases will be discussed in the next section.

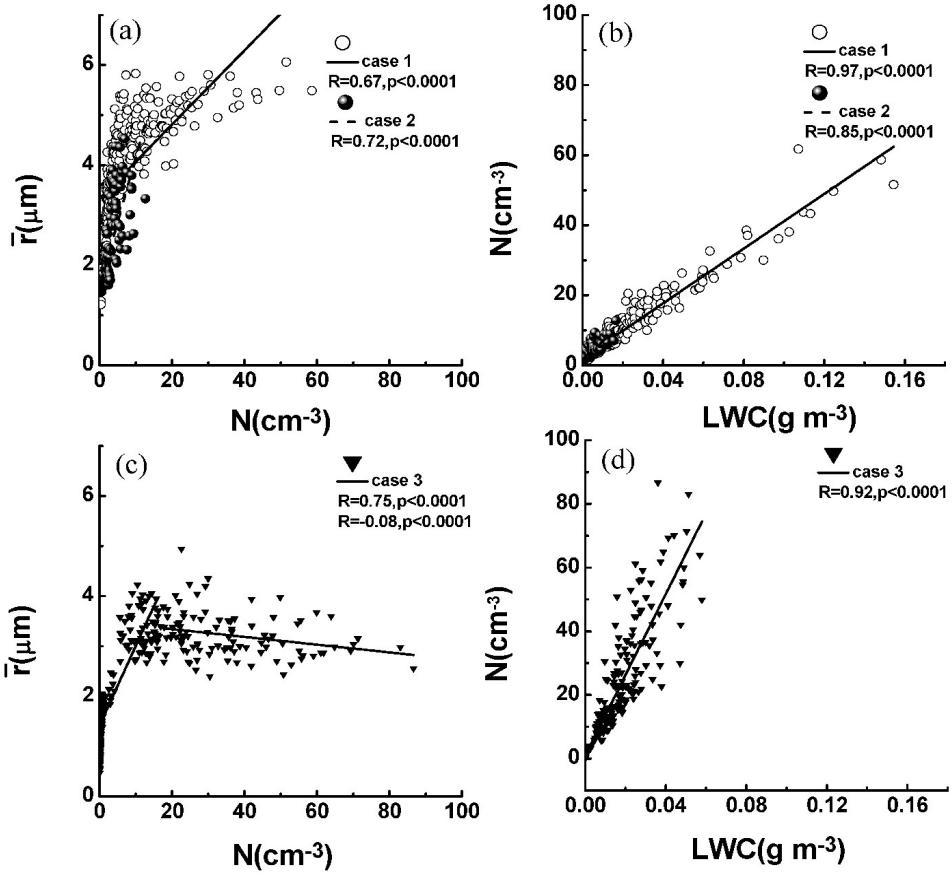

Figure 5. Average radius $\bar{r}$ as a function of N (a, c) and N as a function of LWC (b, d) during the fog case 1, 2 and 3.

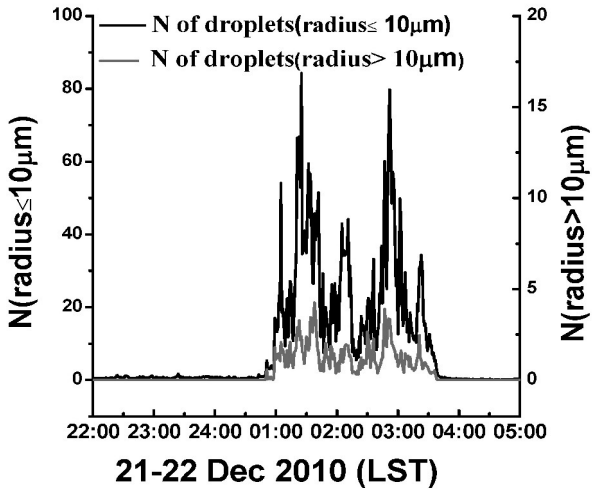

Figure 6. The temporal evolutions of small droplet (radius ≤ 10μm) , big droplet (radius ＞10μm) number concentrations in Xuanen fog case 3.

3.3 *Analysis of the major microphysical process at different stages*

At different stages of fog, there are different characteristics of correlation between the microphysical properties (Niu et al.[5]). Fig.2 shows that the three fog events are strong enough to have their development, mature and dissipation stages, in spite of their short life. Hence analysis will be conducted toward the correlation of the microphysical properties at the different stages of the three fog cases. Fig.7 shows that the microphysical property of the three cases varies over time. According to the change of surface visibility and LWC, the fog process is divided into development, mature and dissipation stages: on December 9, the development stage in case 1 is from 06:15 to 06:50, the mature stage from 06:51 to 08:10, the dissipating stage from 08:11 to 09:40; on December 20, the development stage in case 2 is from 02:40 to 03:10, the mature stage from 03:11 to 03:54, the dissipating stage from 03:55 to 04:50; on

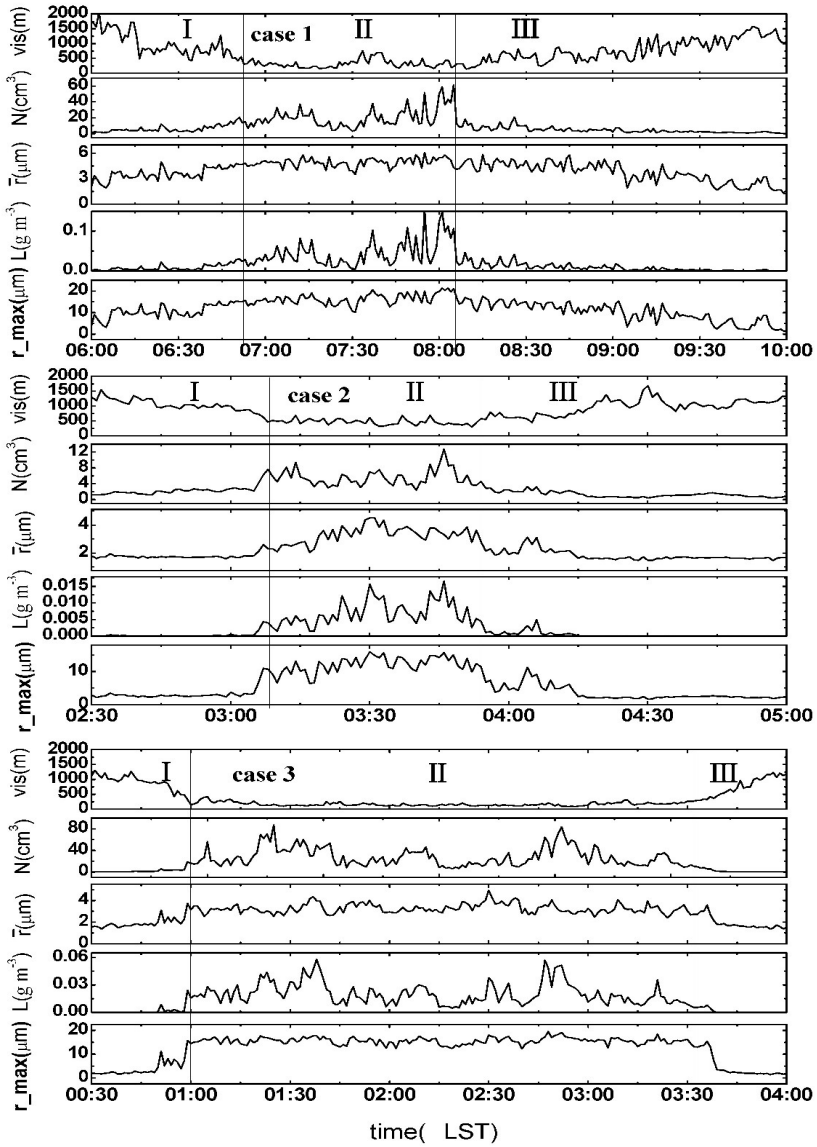

Figure 7. The temporal variations of visibility (VIS), N, $\bar{r}$, liquid water content (L) and maximum radius (r_max) of dense fog case 1, 2 and 3. **Ⅰ** : development stage; **Ⅱ**: mature stage ; **Ⅲ**: dissipation stage.

December 22, the development stage in case 3 is from 00:40 to 01:00, the mature stage from 01:01 to 03:30, the dissipating stage from 03:31 to 04:00.

Figure 8 shows the correlation of the three cases of $\bar{r}$–N and N-LWC at the three stages. It can be observed that at the development and dissipation stages in the three cases, $\bar{r}$–N and N-LWC show obvious positive correlation. The activation of particle and its subsequent growth of condensation will lead to the growth of N and LWC at the same time, whereas the evaporation to deactivation of the particle may lead to the decrease of N and LWC simultaneously. Therefore, the positive correlation of microphysical properties indicates that the activated growth by condensation and evaporation are the most important microphysical process in Xuanen MRF. It is considered when radiation fog enters the mature stage, the collision-coalescence process will cause the decrease of small droplets and the increase of big droplets (Niu et al.[5]). As a result, the positive correlation of $\bar{r}$–N will be weakened to non-correlation or even negative correlation. Seen from Fig.8, the correlation coefficients of the mature stage in the three cases are smaller than that of the other stages. In order to make sure whether the collision-coalescence process in Xuanen MRF event was the major microphysical process, Fig.9 is presented to indicate the temporal evolutions of the threshold function T (Liu et al.[33]) in fog case 1 and 3, with the T value ranging from 0 to 1. "0" means that no collision-coalescence has occurred while "1" means the efficiency of collision-coalescence is up to 100%. The T value for fog case 2 approximates to 0, which indicates that the collision-coalescence process was very weak in this case, or even that process existed at all. In accordance with Liu, the auto conversion parameterizations that have been developed can be generically written as[33]:

$$P = P_0 T \tag{1}$$

where P is the auto conversion rate, P_0 is the rate function describing the conversion rate after the onset of the auto conversion process, and T is the threshold function describing the threshold behavior of the auto conversion process. The size truncation function, employed to quantify the effect of truncation the cloud droplet size distribution on the auto conversion rate, can be used as a threshold function to represent the threshold behavior associated with the auto conversion process, providing a physical basis for the threshold function. The expression of T can be described by:

$$T = \frac{P}{P_0} = \left[\frac{\int_{r_c}^{\infty} r^6 n(r)dr}{\int_{0}^{\infty} r^6 n(r)dr}\right]\left[\frac{\int_{r_c}^{\infty} r^3 n(r)dr}{\int_{0}^{\infty} r^3 n(r)dr}\right] \tag{2}$$

where r is the droplet radius, n (r) is the cloud droplet size distribution, and r_c is the critical radius for auto conversion. On the basis of Liu et al.[33], r_c can be predicted in the auto conversion parameterization and it can be expressed as:

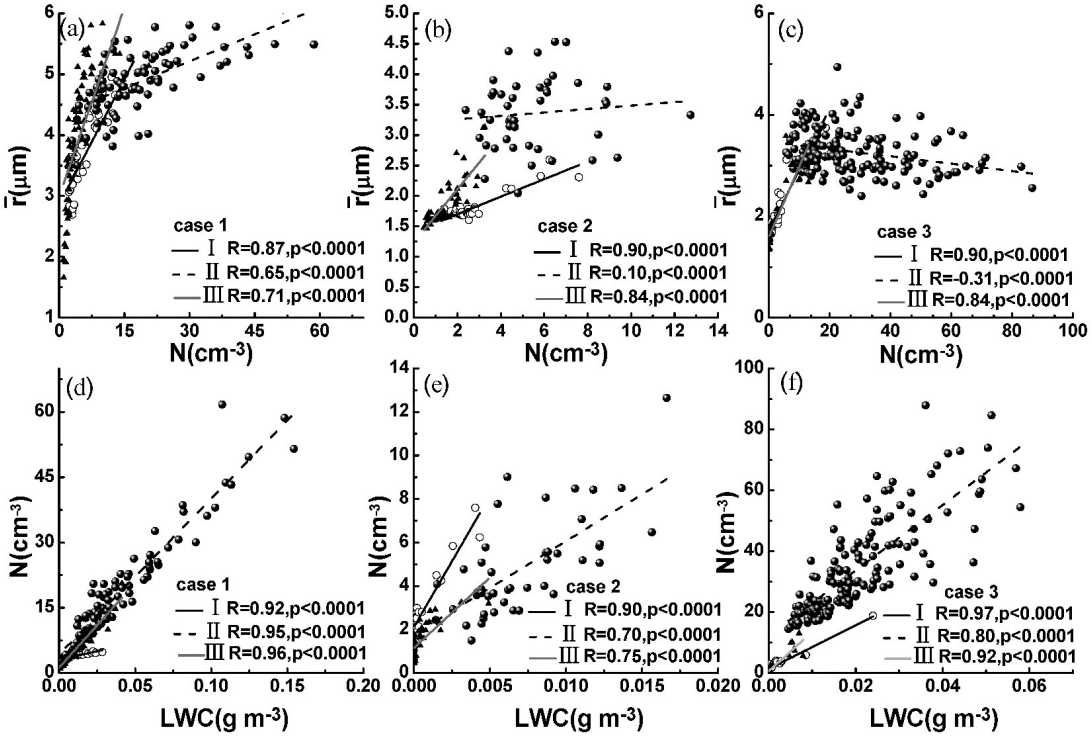

Figure 8. r as a function of N (a, b, c) and N as a function of LWC (d, e, f) during the three stages (Ⅰ-Ⅲ) of three fog cases respectively.

$$r_c \approx 4.09\times10^{-4}\beta_{con}^{1/6}\frac{N^{1/6}}{L^{1/3}} \quad (3)$$

where β_{con}=1.15 $\times10^{23}$ is an empirical coefficient. According to Fig.9, the T value for fog case 1 was relatively high and close to that for the Nanjing radiation fog. In contrast, the T value for fog case 3 was relatively low, with the highest value no higher than 0.22. In addition, the collection efficiencies of auto-conversion process affect mainly large cloud droplets with diameters > 15 μm but not the small ones. Fig.10 shows the temporal evolutions of small droplets (radius ≤ 10 μm) and big droplets (radius>10 μm) number concentrations in the fog case 1 and 2, and case 3 can be seen in Fig.6. The peak value of big droplets in case 1 is around 12/cm^3, and that in case 2 and 3 is no more than 5/cm^3. Due to the low number of large droplets, the collision process became extremely slow in case 2 and 3 in Xuanen. Seen from Fig.8a, b and c, the weakened positive correlation of $\bar{r}-N$ in the mature stage of case1 is mainly caused by the collection process; but in case 2 and 3, this cannot be caused by collection.

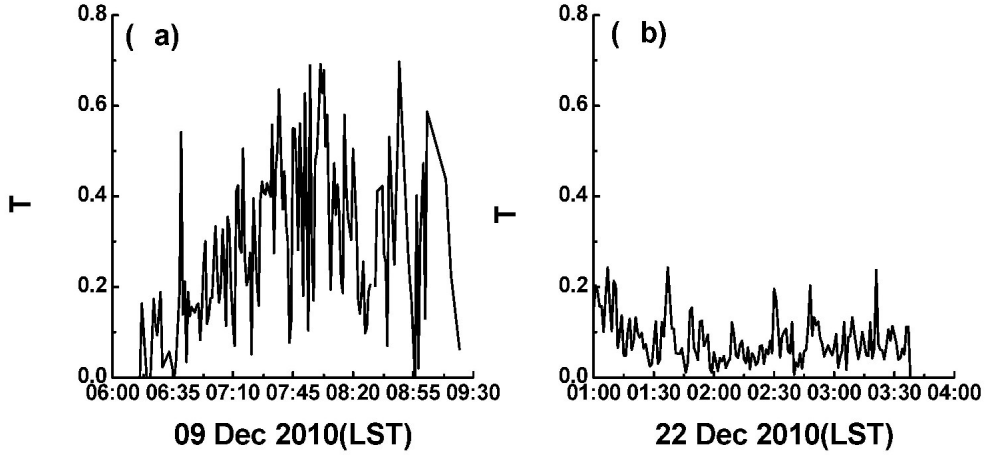

Figure 9. The temporal evolutions of threshold function of fog case 1 (a) and 3(b).

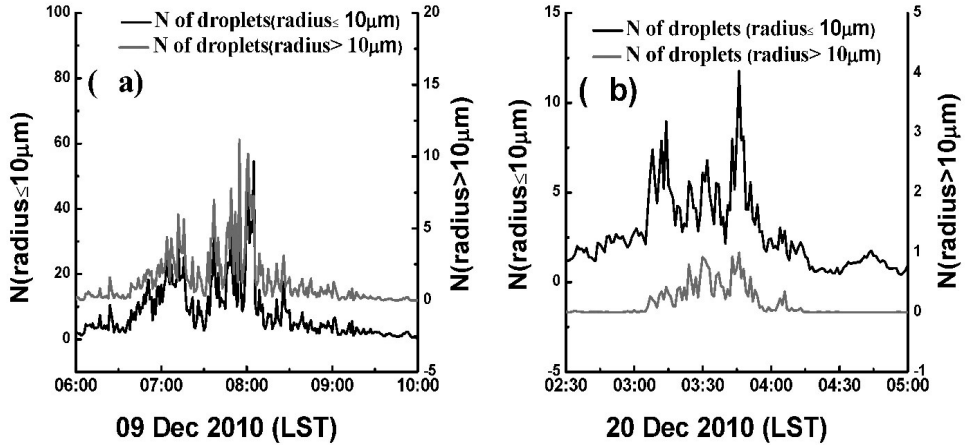

Figure 10. The temporal evolutions of small droplet (radius ≤ 10μm) , big droplet (radius ＞10μm) number concentrations in Xuanen fog case1 (a) and 2 (b).

Figure 11 shows the changes in dew point temperature, air temperature (2 m), ground surface temperature, grass surface temperature and soil temperature (5, 10 ,15 and 20 cm deep, respectively) in case 2 and 3. We can find that the ground and grass surface temperature increased about 4℃ after fog is formed, and it is higher than dew point. This means that evaporation is likely the main process in the mature stage in case 2 and 3. Actually, droplets smaller than 6–8 μm can quickly evaporate and this can be seen from Figs. 6 and 10. The small droplet number concentration during the mature stage of case 2 and 3 rapidly decreased, but no significant change is with big droplet number concentration, maybe due to the evaporation process in case 2 and 3 which can only consume small droplets, but without much influence on the big droplets. Lu pointed out that turbulence could significantly enhance the collision rate for cloud

droplets (> 10 μm in radius)[36]. Therefore, in addition to the evaporation process, the turbulence may reproduce big droplets to compensate for the loss caused by evaporation. As we know the $\bar{r}$ is mainly determined by big droplets. Thus the droplet number significantly decreased but the mean drop diameter did not change significantly in case 2 and 3 in the mature stage. This may be the main reason leading to the weakened positive correlation of $\bar{r}$–N in the mature stage of case 2 and 3.

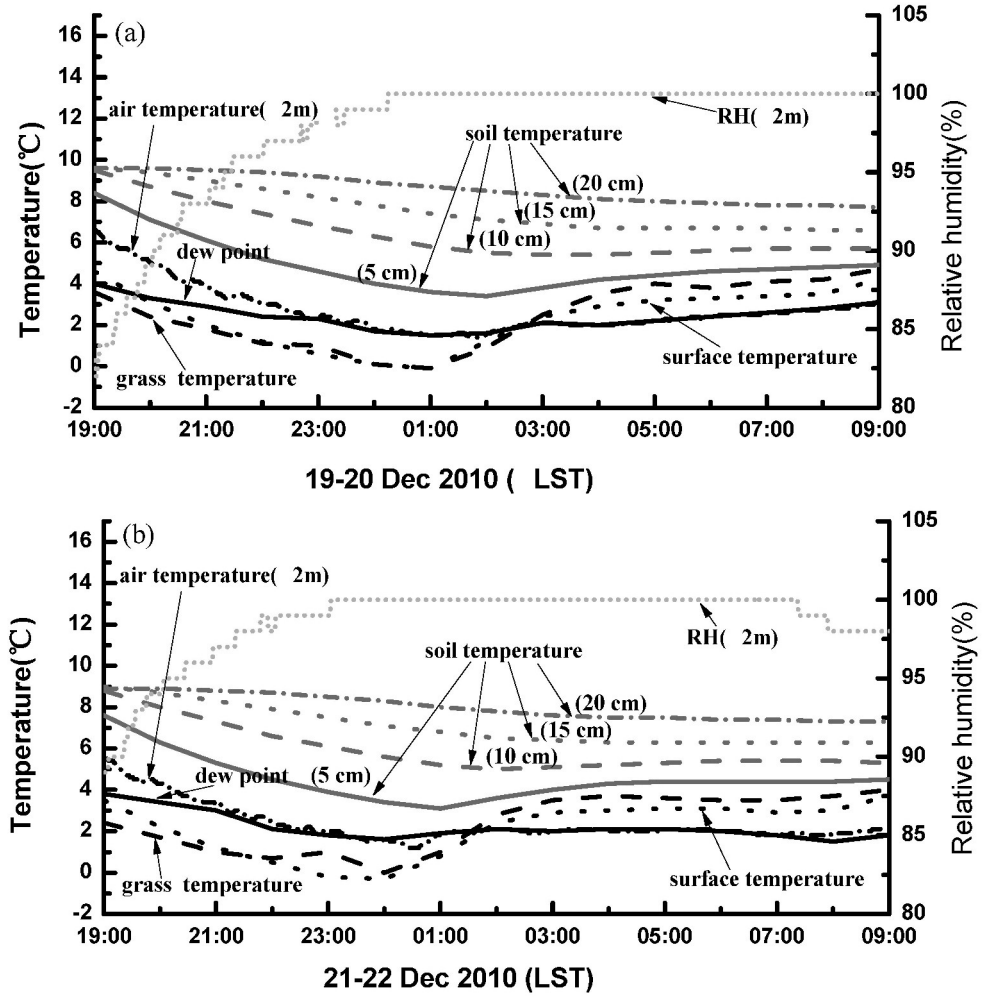

Figure 11. Temporal variations of air temperature at 2 meters above the earth surface, earth surface temperature, dew-point temperature, grass temperature, relative humidity and soil temperature in Xuanen mountainous radiation fog (a) case 2 and (b) case 3, 2010.

It is worth noting that the radiation fog in case 2 and 3 dissipated between 4:00 and 5:00 LST in the early morning. Generally speaking, however, radiation fog is dissipated after sunrise, when solar radiation heats the ground surface which will launch long-wave radiation, the air near the ground will be heated to evaporate the fog droplet. On the other hand, water vapor evaporated from the dew on the ground vegetation after sunrise can help promote and maintain the formation of fog (Pilié et al.[16]). When case 2 and 3 dissipated between 4:00 −5:00 LST, there is no heat from the solar radiation toward the ground surface in this region. The heat fluxes are strongest for case 2 and 3 during the first part of the night, as temperature gradients are strongest between the 2 meters above the ground, the surface, −5, −10, −15, −20 cm. The heat fluxes in the upper soil layers decreased slightly in the late part of the night in both cases. The increase of the surface and grass temperature started at 01:00 LST for case 2 and at about 00:00 for case 3. As the real fog episodes occurs 1 or 2 h later it is to be expected that an elevated cloud layer appeared over the observation site. The profiles of relative humidity and temperature of case 2 and 3 are demonstrated by Fig.12. The relative humidity at the upper level of both cases reached 90% around 00:00. Its downward directed longwave radiation flux heated the surface and compensates the longwave emission from the ground. In Xuanen mountains, the heating effect is very prominent, as the air temperature of the ground surface increases

around 4℃ after fog is formed. It is very unlikely for the advection of warmer air to appear as the dew point kept almost constant during the night. Before 02:00, for both cases, the grass temperature was not as large as dew point, suggesting that dew appeared on the grass during the first part of the clear nights. After 02:00, the grass temperature was larger than dew point. By the heating effect of upward soil flux and downward longwave radiation flux, the dew on the grass was evaporated. In contrast with Figs.9 and 10, we found that the second peak of both small and big droplet concentration appeared at 03:40 for case 2 and at about 03:00 for case 3. This indicates that the dew evaporation has great effect on promoting and maintaining the radiation fog life in Xuanen. With the heat fluxes in the upper soil layers decreasing slightly in the late part of the night, the temperature of grass and surface increased slowly and kept almost constant after 03:40 for case 2 and about 03:00 for case 3. We found that the dissipation time coincides with the time when the grass temperature reaches the peak value. When the upward soil heat flux weakens, the grass temperature stops increasing. The dew evaporation rate should be decreased and the water vapor no longer maintains saturated. The fog, therefore, dissipates.

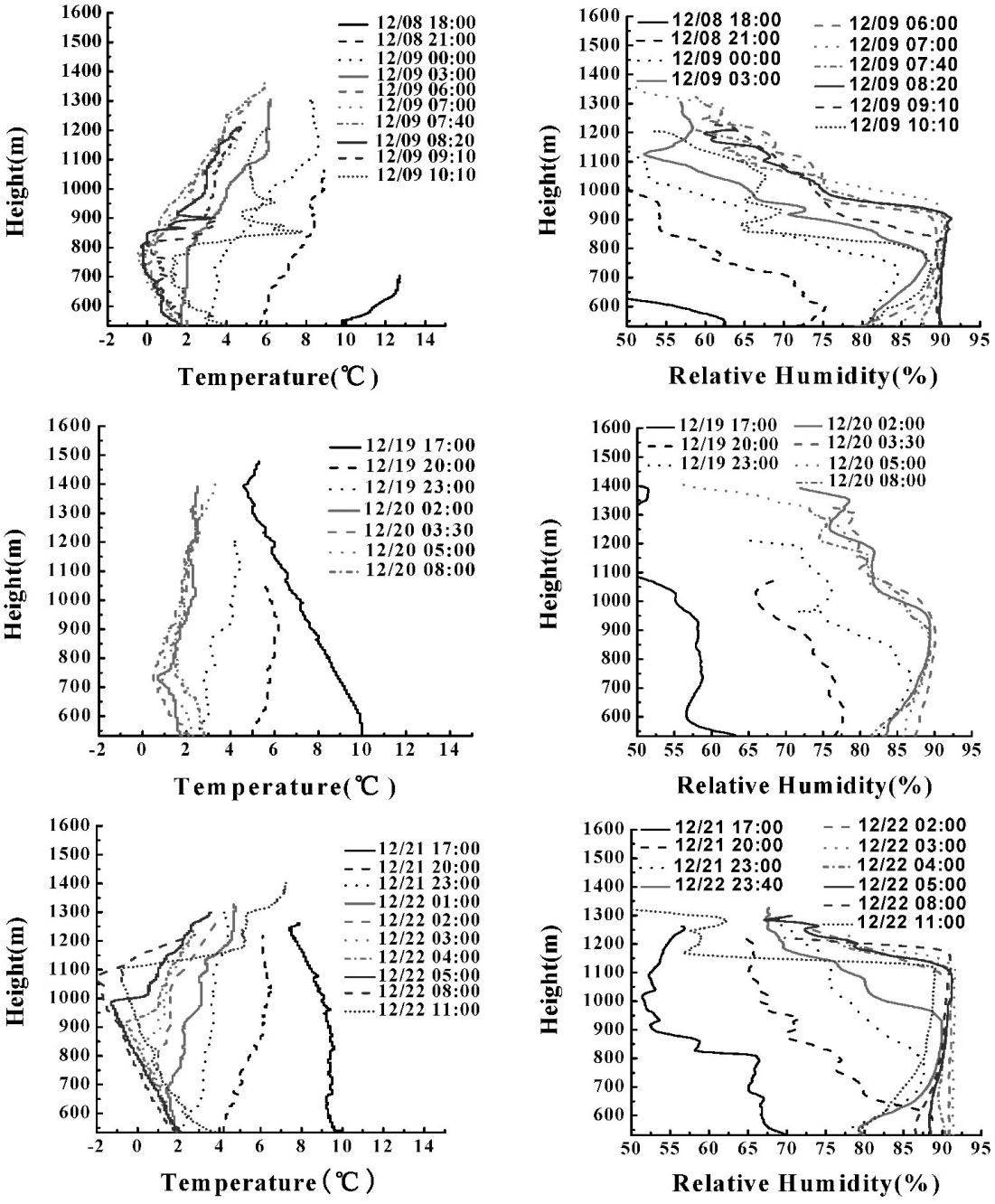

Figure 12. Profiles of temperature and relative humidity of fog case 1, 2 and 3.

4 EVOLUTIONARY PROPERTIES OF FOG DROPLET SPECTRA

Figure 3 has already given the average fog droplet size distribution of the three fog events observed at Xuanen. This section mainly deals with the evolutionary properties of fog droplets in different stages. Fig. 13 shows the distribution properties of the fog droplet in the three MRF events observed at Xuanen in the development, mature and dissipation stage respectively. It can be seen from Fig. 13 that Xuanen MRF displays relatively low number concentration in each size class, less than 1 /(cm^3 μm), during the development stage. In the mature stage, small droplet number concentration increases to 10/(cm^3 μm) and reaches the peak at 20 μm. It needs to be noted that big droplets were formed as early as in the development stage in Xuanen MRF events, which is clearly manifested in Figs.7 and 10. Specifically, when the visibility was between 800 and 1,000 meters, fog droplets of over 20 μm in diameter were formed in both three fog cases.

Generally speaking, some big droplets grow by collecting small ones, and in radiation fog events they usually appear in the mature stage when visibility is the lowest (Niu et al.[5]; Liu et al.[29]) rather than in the development stage when visibility is relatively high. It can be seen from Figs.6 and 10 that big droplets and small droplets appeared almost simultaneously in the development stage in Xuanen MRF events. At the beginning stage in fog case 1 and 3, big droplet number concentration was 2–3/cm^3 while in fog case 2, its big droplet number concentration was 1/cm^3. When analyzing the fog event in Peoria, Illinois (USA), Westcott et al.[34], pointed out that with low clouds in place, the cloud base would keep expanding until it reaches the underlaying surface while the cloud top radiation cooling would trigger the turbulent mixing process starting from cloud top and send clouds of lower temperatures below the cloud base via turbulence [34]. Observation of Paris fog events by Degefie et al. reveals that when low clouds existed, big droplets did transport low-temperature clouds to below the cloud base, and that evaporation of big droplets transported vapor to the air below the cloud base, hence facilitating the condensation and activation process and the formation of fog droplets [35]. As can be seen in Fig.12, the temperature profiles of case 2 and 3 were unstable stratification before the fog was formed. Thermal instability can lead to turbulence. The formation big droplets larger than 20 μm in diameter in Xuanen MRF events when visibility was between 800 and 1,000 meters was very likely to result from turbulent movement of low cloud base to earth surface. The observation showed that Xuanen MRF started with low clouds, which formed fog droplets when they reached earth surface. This result is consistent with the observation of Westcott and Degefie, and quite different from other MRF in China[34, 35].

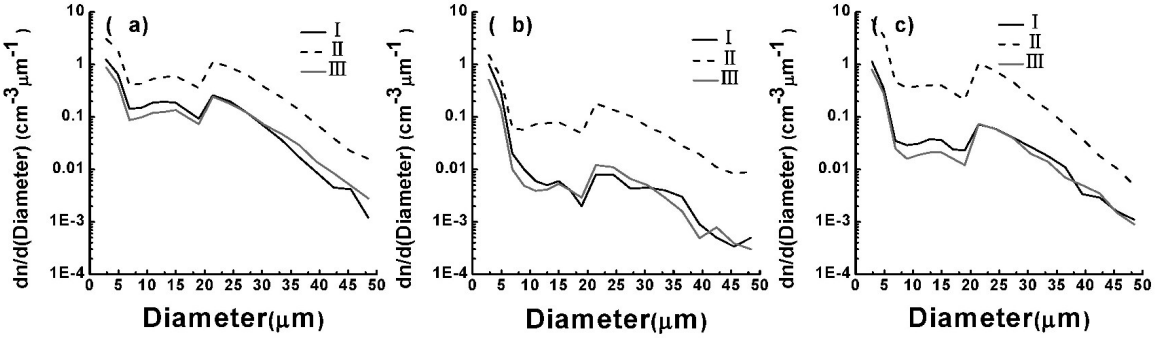

Figure 13. Average spectra of the three stages (Ⅰ-Ⅲ) as defined in Fig.5 of the dense fog events (a : case 1, b: case 2, c: case 3).

5 CONCLUSIONS

Based on the fog droplet spectra, visibility and boundary layer meteorological variables of three fog events observed at Xuanen in the winter of 2010, this paper analyses Xuanen mountains radiation fog's microphysical process and its temporal evolutions and compares the results with those observed in other areas. The major conclusions are as follows:

(1) The observed radiation fogs in Xuanen mountainous region lasted no more than 3 hours. Only one fog event recorded a minimum visibility of 100 m, and no extremely dense fog occurred. The average liquid water content in these fog events was between 0.000,8–0.004 g/m^3 and the number concentration was between 58–85/cm^3, smaller than that in urban and other mountainous regions. A clean background led to low concentrations of aerosol particles, which resulted in smaller number concentration of fog droplets compared with that in other areas.

(2) The liquid water content, mean radius and number concentration in Xuanen MRF events were positively correlated, especially during the development and dissipation stages, which reveals that condensation

and evaporation were the major microphysical processes in these fog events. Threshold function of fog case 2 and 3 shows that collision-coalescence process does not occur in all radiation fog cases at this region. During the mature stage an important fog layer is present and strong super-saturation no longer occurs. The fog droplets are in a water vapor environment that oscillates quietly around its saturation value. Under these conditions larger droplets are rather inert and do only mildly change their size. Droplets smaller than 6−8 μm, however, can now quickly evaporate but new super-saturations will be insufficient for them to become a fog droplet again. Thus the droplet number will decrease but the mean drop diameter does not change significantly.

(3) Upper-level temperature inversion resulting from the interaction between low clouds top radiation cooling and downward long-wave radiation heating, together with poor ventilation in the Xuanen observation site, made upward soil heat flux significant in midnight. Earth surface and grass temperature increased by 4℃ around 03:00 −04:00, compared with those measured before the fog came into existence, which differed obviously from other mountainous regions and urban areas in the formation of radiation fogs. It was also observed that Xuanen MRF dissipated at night. The dissipation time coincided with the time when the grass temperature reached the peak value, which indicated that dew evaporation is a key role in maintaining the Xuanen MRF. When the upward soil heat flux weakens, the grass temperature stopped increasing. The dew evaporation rate should be decreased and the weakened water vapor was no longer to maintain saturation. The fog, therefore, dissipates.

(4) With visibility being 1,000 m, liquid water content in Xuanen MRF was measured to be 0.01 g/m^3, which differed greatly from that observed in Nanjing and other urban areas. In Nanjing, such a value could not be measured before visibility reduced to less than 100 m. It can be seen from the analysis of the microphysical properties of radiation fog events and the temporal evolutions of their size distribution that big droplets larger than 20 μm in diameter were formed in the development stage and that their number concentrations were between 2 −3/cm^3, which can explain why more liquid water content was observed in the development stage of Xuanen MRF events.

Acknowledgement: We thank the Xuanen Meteorological Bureau of Hubei province, China for their support during the field campaign and for providing meteorological data.

REFERENCES:

[1] GULTEPE I, TARDIF R, MICHAELIDES S C, et al. Fog research: A review of past achievements and future perspectives [J]. Pure Appl Geophys, 2007, 164 (6): 1121-1159.

[2] GUO X and ZHENG G. Advances in weather modification from 1997 to 2007 in China [J]. Adv Atmos Sci, 2009, 26 (2): 240-252.

[3]BENDIX J, ROLLENBECK R, GÖTTLICHER D. Seasonality and diurnal pattern of very low clouds in a deeply incised valley of the eastern tropical Andes (South Ecuador) as observed by a cost-effective WebCam system [J]. Meteorol Appl, 2008,15: 281-291.

[4] NIU S J, LU C S, LIU Y G, et al. Analysis of the microphysical structure of heavy fog using a droplet spectrometer: a case study [J]. Adv Atmos Sci, 2010, 27 (6): 1259-1275.

[5] NIU S J, LU C S, YU H Y, et al. Fog research in China: an overview [J]. Adv Atmos Sci, 2010, 27(3): 639-662.

[6] PINNICK R G, HOIHJELLE D L, FEMANDEZ G, et al. Vertical structure in atmospheric fog and haze and its effects on visible and infrared extinction [J]. J Atmos Sci, 1978, 35: 2020-2032.

[7]GULTEPE I, MILBRANDT J A.Microphysical observations and mesoscale model simulation of a warm fog case during FRAM project [J]. Pure Appl Geophys, 2007, 164: 1161-1178.

[8] GARCí A- GARCí A F, VIRFUENTES U, MONTERO-MARTí NEZ G. Fine-scale measurements of fog-droplet concentrations: A preliminary assessment [J]. Atmos Res, 2002, 64: 179-189.

[9] GERBER H E. Microstructure of a radiation fog [J]. J Atmos Sci, 1981, 38, 454-458.

[10] GERBER H E. Supersaturation and droplet spectral evolution in fog [J]. J. Atmos. Sci., 1991, 48: 2569-2588.

[11] FUZZI S, FACCHINI M C, ORSI G, et al. The Po Valley fog experiment 1989: An overview [J]. Tellus, 1992, 44B, 448-468.

[12] GOODMAN J. The microstructure of California coastal fog and stratus [J]. J Appl Meteorol, 1977, 16 (10), 1056-1067.

[13] ZHOU B B, and FERRIER B S. Asymptotic analysis of equilibrium in radiation fog [J]. J Appl Meteorol Climatol, 2008, 47: 1704-1722.

[14] HUANG Yu-sheng, HUANG Yu-ren, LI Zi-hua, et al. The microphysical structure and evolution of winter fog in Xishuangbanna [J]. Acta Meteorol Sinica, 2000, 55(6): 715-725 (in Chinese).

[15] TANG Hao-hua, FAN Shao-jia, WU Dui, et al. Research of the microphysical structure and evolution of dense fog over Nanling Mountain area [J]. Acta Sci Nat Univ Sunyatseni, 2002, 41(4), 92-96 (in Chinese).

[16] PILIé R J, MACK E J, KOCMOND W C, et al. The life cycle of valley fog, Part II: Fog Microphysics [J]. J. Appl Meteorol, 1975, 14: 364-374.

[17] PILIé R J, MACK E J, KOCMOND W C, et al. The life cycle of valley fog, Part I: Micrometeorological characteristics [J]. J Appl Meteorol, 1975, 14: 347-363.

[18] HOLETS S, SWANSON R N. High-inversion fog episodes in Central California [J]. J Appl Meteorol 1981, 20: 890-899.

[19] FITZJARRALD D R, LALA G G. Hudson valley fog environments [J]. J Appl Meteorol 1989, 28: 1303-1328.

[20] WOBROCK W, SCHELL D, MASER R, et al. Meteorology characteristics of the Po Valley fog [J]. Tellus, 1992, 44B: 469-488.

[21] DENG X J, WU D, SHI Y Q, et al. Comprehensive

analysis of the macro- and micro-physical characteristics of dense fog in the area south of the Nanling Mountains [J]. J Trop Meteorol, 2008, 14(1): 11-14.

[22] HE You-jiang, ZHU Bin, MA Li. The physical process of Chongqing fog's genesis and dissipation in winter [J]. J Nanjing Inst Meteorol, 2003, 26 (6): 821-828 (in Chinese).

[23] SHI Y Q, DENG X J, HU Z J, et al. A three-dimensional numerical study on dense fog over mountainous areas [J]. J Trop Meteorol, 2007, 13(1):17-20.

[24] WU D, WU X J, LI F, et al. Long-term variations of fog and mist in mainland China during 1951-2005 [J]. J Trop Meteorol, 2013, 19(2): 181-187.

[25] GUO, L J, GUO X L, FANG C G, et al. Observation analysis on characteristics of formation, evolution and transition of a long-lasting severe fog and haze episode in North China [J]. Sci China: Ear Sci, 2015, 58: 329-344, doi: 10.1007/s11430-014-4924-2.

[26] YANG Zhong-qiu, Xu Shao-zu, GENG Biao. Formation and microphysical structure of sea fog in spring in Zhoushan area [J]. Acta Oceanol Sinica, 1989, 11 (4): 421-438 (in Chinese).

[27] ZHANG Shu-ting, NIU Sheng-jie, ZHAO Li-juan. The Microphysical Structure of a Sea Fog Event in the South China Sea [J]. Chin J Atmos Sci, 2013, 27 (3): 552-562 (in Chinese).

[28] JEREMY P. Radiation Fog. Part Ⅰ: Observations of stability and drop size distributions [J]. Boundary-Layer Meteorol, 2011, 139:167-191.

[29] LIU D Y, YANG J, NIU S J, et al. On the evolution and structure of a radiation fog event in Nanjing [J]. Adv Atmos Sci, 2011, 28(1), 223-237.

[30] LI Zi-hua, HUANG Jian-ping, ZHOU Yu-quan, et al. Physical structures of the five-day sustained fog around Nanjing in 1996 [J]. Acta Meteorol Sinica, 1999, 57(5): 622-631 (in Chinese).

[31] HUANG Yu-sheng, HUANG Yu-ren, LI Zi-hua, et al. The microphysical structure and evolution of winter fog in Xishuangbanna [J]. Acta Meteorol Sinica, 2000, 55(6): 715-725 (in Chinese).

[32] LU C S, LIU Y G, NIU S J, et al. Examination of microphysical relationships and corresponding microphysical processes in warm fogs [J]. Acta Meteorol Sinica, 2013, 27(6), 832-848.

[33] LIU Y, DAUM P H, MCGRAW R L. Size truncation effect, threshold behavior, and a new type of auto conversion parameterization [J]. Geophys Res Lett, 2005, 32, L11811, doi:10.1029/2005GL022636.

[34] WESTCOTT N E, and KRISTOVICH D A R. A climatology and case study of continental cold season dense fog associated with low clouds [J]. J Appl Meteorol Climatol, 2009, 48(11), 2201-2214.

[35] DEGEFIE D T, El-MADANY T-S, HEJKAL J, et al. Microphysics and energy and water fluxes of various fog types at SIRTA, France [J]. Atmos Res, 2014, doi: 10.1016/ j.atmosres.2014.03.016.

Citation: FEI Dong-dong, NIU Sheng-jie and YANG Jun. Analysis of the microphysical structure of radiation fog in Xuanen mountainous region of Hubei, China [J]. J Trop Meteorol, 2017, 23(2): 177-190.